

Anthropomorphic Finger Mechanism with a non-elastic Branching Tendon

Kazuya Yanagisawa, Shouhei Shirafuji, Shuhei Ikemoto, Koh Hosoda *

Information Science and Technology, Osaka University
yanagisawa.kazuya@ist.osaka-u.ac.jp

Abstract. To realize both grasp stability and manipulation dexterity is a central problem in the development of robot hands. In recent years, many underactuated robot hands have been developed that flexibly conform to an object's surface with simple control.

In contrast, it is difficult to realize dexterous manipulation by such underactuated hands in which all degrees of freedom (DoFs) should be controlled. In this research, to realize the dexterous manipulation by simple mechanism and control, we develop a robot gripper comprising of two tendon-driven robotic fingers with non-elastic branching tendons. The branching tendon is a tendon that branches out and connects an actuator to different links. The two joints of this robotic finger are coupled by the non-elastic branching tendon when no external force is exerted. If sufficient external force is applied to the fingertip, one of the tendons slackens and the coupling between the two joints is lost. This means that the two-DoF robotic finger is easily controlled as a single DoF mechanism when reaching toward an object, but when the fingertip is placed on the object, the coupling provided by the branching tendon is released and the finger shifts. Based on this idea, we develop and control a two-DoF robotic finger equipped with two tendons including a non-elastic branching tendon. We also analyse the conditions, where the branching tendon slackens, and confirmed in an experiment. As the result, the availability of controlling the slack of branched tendon was successfully confirmed.

1 Introduction

Humanlike stability and dexterous object manipulation has been a central focus in robotic hand research. The hardware of robot hands is designed in two ways; by actuating joints directly by motors and by actuating joints through tendons. When a robot hand is designed to imitate a compact human's hand, a tendon-driven mechanism is often employed since it does not necessarily put motors at the joints. Examples of tendon-robotic hands are JPL/Stanford Hand[1], Utah/MIT Hand[2] and DLR-Hand[3] are all employing the tendon-driven mechanism. In particular, ACT Hand[4] has very similar musculotendinous structure to a human hand. A sufficient versatile dexterous robot hand requires many degrees of freedom(DoFs). To achieve such versatility, the system must control

* This work was supported by JSPS KAKENHI Grant Numbers 23650098, 24-3541.

more tendons than joints; that is, it must control the number of DoFs. As the number of DoFs increases, controlling becomes increasingly complex.

To overcome this problem, a hand which has less actuators, which is called an underactuated mechanism, has been researched[5]. For example, Soft Gripper, which realizes flexible encapsulation grasping[6] and 100G Hand, which accomplishes a fast catching task[7]. These hands can be simplified because they replace actuators with passive mechanical elements such as springs. TUAT/Karlsruhe Hand has five underactuated fingers comprising rigid linkages and is capable to realize various types of grasping[8]. However, an underactuated hand is often designed to be specialized for specific tasks because it basically has less DoFs.

In real human hands, the distal extensor tendon branches before the proximal interphalangeal joint (PIP joint). Shirafuji et al. focused on this fact, and developed a three-DoF robotic finger with a branching tendon structure[9]. If the branching tendon is non-elastic, two joints are geometrically constrained when both linkages are tight. When the fingertip touches an object, it receives a certain amount of external force, and the constraint is released as one of the branches slacks. Therefore, the finger can be controlled as a two-DoF mechanism when not touching an object and as a three-DoF mechanism when touching an object.

Despite the expected utility of non-elastic branching tendons in the robot hands, the desired magnitude of the external force and tensions in the tendons that will alter the configuration, and the application of the mechanism to object manipulation tasks, has not been clarified. In the branching tendon mechanisms investigated by Sawada et al., elastic tendons were assumed and slack was not considered[10].

In this research, we develop a robot gripper consisting of two-DoF fingers with non-elastic branching tendons to realize stable grasping and dexterous manipulation. First, we propose a branching-tendon finger mechanism and derive the condition under which one branching tendon slacks. We then develop a two-fingered robot gripper and demonstrate that the finger can be controlled as a one-DoF gripper in the absence of an external force. We also demonstrated that the constraint on the finger is lessened when touching an object, thereby realizing slack control.

2 Kinematics of Manipulator with Non-elastic Branching Tendon

Fig. 1 is a schematic illustration of the proposed robotic finger, which has two-DoF and two tendons denoted as tendon 1 and tendon 2. The tendons are assumed non-elastic. A branching point placed between joint 1 and the corresponding actuator splits tendon 2 through two routings, denoted as tendon 2a and 2b. One of the divergent tendons is attached to the link connecting joints 1 and 2, the other is attached to the end link. The motions of both manipulator joints are coupled by the geometric constraint generated by the branching tendon under certain conditions. This section briefly discusses the kinematics of the manipulator with one non-elastic branching tendon, and derives the condition that

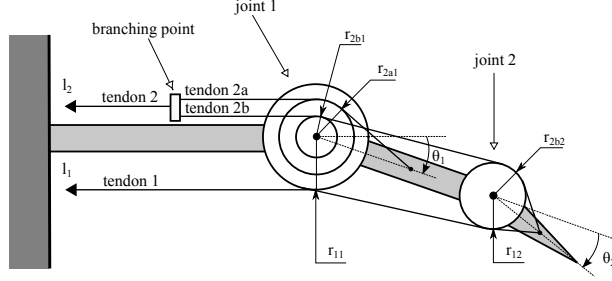


Fig. 1. Robotic finger with two-DoFs and two tendons. One of the tendons branches at the branching point.

maitains the coupled motion of both joints. In the tendon-driven manipulator, the angular velocities of the joints must be related to the tendon displacement velocities. To describe the kinematics, we must also express a general relationship between the end-point velocity and the joint angular velocities. We first relate the vector of tendon displacement velocity $\dot{\mathbf{l}}$ to the vector of joint angular velocity $\dot{\boldsymbol{\theta}}$ as follows:

$$\dot{\mathbf{l}} = \mathbf{P}\dot{\boldsymbol{\theta}}, \quad (1)$$

where \mathbf{P} is the tendon Jacobian matrix, determined by the routing of each tendon. The tensile force on each tendon and joint torque are also related through the matrix \mathbf{P} :

$$\boldsymbol{\tau} = -\mathbf{P}^T \mathbf{f}, \quad (2)$$

where $\boldsymbol{\tau}$ and \mathbf{f} are vectors of joint torques and tensile forces, respectively. If the number of tendons in the manipulator exceeds the number of joints and \mathbf{P} is a column full-rank matrix, the tensile force vector is expressed in terms of the joint torque vector as follows:

$$\mathbf{f} = -\mathbf{P}^+ \boldsymbol{\tau} + \mathbf{f}_b, \quad (3)$$

where \mathbf{P}^+ is the pseudo-inverse of \mathbf{P} and \mathbf{f}_b is its null-space. \mathbf{f}_b is called the bias tensile force. The kinematics of general tendon-driven manipulators is detailed in Kobayashi et al.[11] and in several robotics texts[12, 13]. In the proposed robotic finger, considering the branching tendon as two independent tendons, as shown in Fig. 2. In this case, (1) can be expressed as

$$\begin{bmatrix} \dot{l}_1 \\ \dot{l}_{2b} \\ \dot{l}_{2a} \end{bmatrix} = \mathbf{P} \begin{bmatrix} \dot{\theta}_1 \\ \dot{\theta}_2 \end{bmatrix}, \quad (4)$$

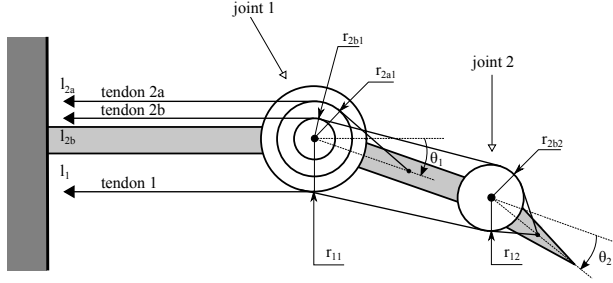


Fig. 2. Model of the proposed robotic finger. The branching tendon in the proposed robotic finger can be considered as two independent tendons.

where l_i is the displacement of each tendon, and the tendon Jacobian matrix is given as:

$$\mathbf{P} = \begin{bmatrix} -r_{11} & -r_{12} \\ r_{2b1} & r_{2b2} \\ r_{2a1} & 0 \end{bmatrix}, \quad (5)$$

where r_{ij} is the moment arm between each tendon and joint (the subscript indicates the corresponding joint and tendon). Note that the positive direction of rotation is counterclockwise in the figure, whereas the positive tendon displacement is the pulling direction. In order to apply any desired torque to each joint, the system has to be tendon controllable depending on elements of the matrix \mathbf{P} [11]. We assume that \mathbf{P} is satisfied the condition to be tendon controllable.

We consider that the manipulator has a branching tendon, as shown in Fig. 1 and discussed above, and investigate the kinematics. The branching tendon has been sometimes adopted in underactuated manipulators[5]. Sawada and Ozawa[10] proposed a generalized control method for a tendon-driven mechanism with branching tendons. Shirafuji et al.[9] suggested that the tendon-driven manipulator with branching tendons can be controlled with fewer DoFs than with the original number of DoFs virtually under the assumption that the branching tendon has no elasticity. This reduction in DoFs is caused by the geometric constraint of the branching tendon that generates coordinated joint motions. In addition, Shirafuji et al. implied that the system can be arbitrarily released from this coupled motion by adjusting the bias tensile force. Here, we apply Shirafuji et al.'s approach[9] to our proposed robotic finger, and derive the conditions under which coupled motion is retained.

Shirafuji et al.[9] use a virtual tendon Jacobian matrix \mathbf{P}_v to represent the relationships between tendons including branched tendons and coupled joints. First, we derive this matrix for the proposed robotic finger. Equation (4) can be

divided as follows:

$$\dot{l}_1 = \mathbf{P}_1 \begin{bmatrix} \dot{\theta}_1 \\ \dot{\theta}_2 \end{bmatrix}, \quad (6)$$

$$\begin{bmatrix} \dot{l}_{2a} \\ \dot{l}_{2b} \end{bmatrix} = \mathbf{P}_2 \begin{bmatrix} \dot{\theta}_1 \\ \dot{\theta}_2 \end{bmatrix}, \quad (7)$$

where \mathbf{P}_1 and \mathbf{P}_2 are the corresponding submatrices, given as:

$$\mathbf{P}_1 = \begin{bmatrix} -r_{11} & -r_{12} \end{bmatrix} \quad \mathbf{P}_2 = \begin{bmatrix} r_{2b1} & r_{2b2} \\ r_{2a1} & 0 \end{bmatrix}. \quad (8)$$

If neither tendon is slackened, the tendon displacement velocities of both tendons branched from tendon 1 has to be the same because they are connected at the same point. Therefore, $\dot{l}_{2a} = \dot{l}_{2b} = \dot{l}_2$ and (7) can be rewritten as:

$$\dot{l}_2 \begin{bmatrix} 1 \\ 1 \end{bmatrix} = \mathbf{P}_2 \begin{bmatrix} \dot{\theta}_1 \\ \dot{\theta}_2 \end{bmatrix}. \quad (9)$$

The joint angular velocity is derived using the inverse of \mathbf{P}_1 as follows:

$$\begin{bmatrix} \dot{\theta}_1 \\ \dot{\theta}_2 \end{bmatrix} = \dot{l}_2 \mathbf{P}_2^{-1} \begin{bmatrix} 1 \\ 1 \end{bmatrix} = \frac{\dot{l}_2}{r_{2a1}} \begin{bmatrix} 1 \\ \frac{r_{2a1}-r_{2b1}}{r_{2b2}} \end{bmatrix}. \quad (10)$$

During completely taut coupled motion, the angular velocities of each joint are related as follows:

$$\dot{\theta}_1 : \dot{\theta}_2 = 1 : \frac{r_{2a1} - r_{2b1}}{r_{2b2}}. \quad (11)$$

Next, we now detail the condition under which the tendons remain taut, and define a virtual angle θ_v that represents the angle of the coupled joints: $\dot{\theta}_v = \dot{l}_2$. Substituting (10) into (4), we obtain

$$\begin{bmatrix} \dot{l}_1 \\ \dot{l}_{2b} \\ \dot{l}_{2a} \end{bmatrix} = \begin{bmatrix} \mathbf{P}_1 \\ \mathbf{P}_2 \end{bmatrix} \dot{l}_2 \mathbf{P}_2^{-1} \begin{bmatrix} 1 \\ 1 \end{bmatrix} = \begin{bmatrix} \mathbf{P}_1 \mathbf{P}_2^{-1} \begin{bmatrix} 1 \\ 1 \end{bmatrix} \\ 1 \\ 1 \end{bmatrix} \dot{\theta}_v. \quad (12)$$

Since $\dot{l}_{2a} = \dot{l}_{2b} = \dot{l}_2$ in the absence of slack, (12) can be rewritten as follows:

$$\begin{bmatrix} \dot{l}_1 \\ \dot{l}_2 \end{bmatrix} = \begin{bmatrix} \mathbf{P}_1 \mathbf{P}_2^{-1} \begin{bmatrix} 1 \\ 1 \end{bmatrix} \\ 1 \end{bmatrix} \dot{\theta}_v. \quad (13)$$

Equation (13) relates the joint angular velocities to the tendon displacement velocity of the tendon-driven manipulator with one-DoF and two tendons. In this case, the tendon Jacobian matrix of the system is

$$\mathbf{P}_v = \begin{bmatrix} \mathbf{P}_1 \mathbf{P}_2^{-1} \begin{bmatrix} 1 \\ 1 \end{bmatrix} \\ 1 \end{bmatrix}, \quad (14)$$

and we call \mathbf{P}_v as virtual tendon Jacobian matrix. Second, we apply this matrix to (2). Multiplying both sides of (2) by $(\mathbf{P}_2^{-1}[1 \ 1]^T)^T$, we obtain:

$$[1 \ 1] \mathbf{P}_2^{-T} \boldsymbol{\tau} = -[1 \ 1] \mathbf{P}_2^{-T} \mathbf{P}^T \mathbf{f} = -\mathbf{P}_v \begin{bmatrix} f_1 \\ f_{2a} + f_{2b} \end{bmatrix}, \quad (15)$$

where f_i denotes the tensile forces and $f_{2a} + f_{2b}$ is equivalent to the tensile force of the branching tendon f_2 . Furthermore, defining the virtual torque vector by

$$\boldsymbol{\tau}_v = [1 \ 1] \mathbf{P}_2^{-T} \boldsymbol{\tau}, \quad (16)$$

we can control the proposed robotic finger regarding as a tendon-driven manipulator with one-DoF and two tendons virtually under the assuming that there is no slack of the tendons.

On the other hand, the coupled motion is lost when one of the divided tendons becomes slack. Slackening is induced by the forces applied to the robotic finger, including the external forces generated by contact with the environment and inertial forces during finger motion. The proposed robotic finger has a branching tendon, and slackness permits two states of tendons, as shown Fig. 3. These states can be used for controlling the robotic finger without coupled joint motions (for instance, when the finger manipulates a grasped object using its end link). Therefore, we finally derive a condition that one of the tendons divided from the branching tendon slackens when an external force applied to the fingertip supplies torque to the joints. This situation is shown in Fig. 4 Considering a planar motion, and given the external force applied to the robotic fingertip by the vector \mathbf{F} , the joint torques are related to the external force as

$$\boldsymbol{\tau} = \mathbf{J}^T \mathbf{F}, \quad (17)$$

where \mathbf{J} is a Jacobian matrix relating the velocity of the contact point in each direction to each joint angular velocity. Assuming frictionless point contact, the external force vector can be described as $\mathbf{F} = [0 \ F]^T$, and (17) can be written as:

$$\boldsymbol{\tau} = \begin{bmatrix} L_1 \cos \theta_1 + L_2 \cos(\theta_1 + \theta_2) \\ L_2 \cos(\theta_1 + \theta_2) \end{bmatrix} F, \quad (18)$$

where L_1 is the length of the link between the joints and L_2 is the distance between the contact point and joint 2. Because tendons exert no pushing motion, they slacken when their tensile force becomes negative. Therefore, substituting (18) into (3), we obtain

$$\begin{bmatrix} f_1 \\ f_{2b} \\ f_{2a} \end{bmatrix} = -\mathbf{P}^+ \begin{bmatrix} L_1 \cos \theta_1 + L_2 \cos(\theta_1 + \theta_2) \\ L_2 \cos(\theta_1 + \theta_2) \end{bmatrix} F + \mathbf{f}_b, \quad (19)$$

where the branching tendon is considered as two independent tendons (see Fig. 4). When either f_{2b} or f_{2a} becomes negative under the external force F and the

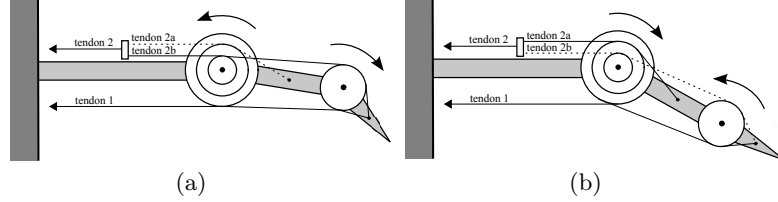


Fig. 3. States of the tendons when one tendon is slack. The slackened tendon is indicated by the dotted line. (a) The state when tendon 2a is slack. (b) The state when tendon 2b is slack.

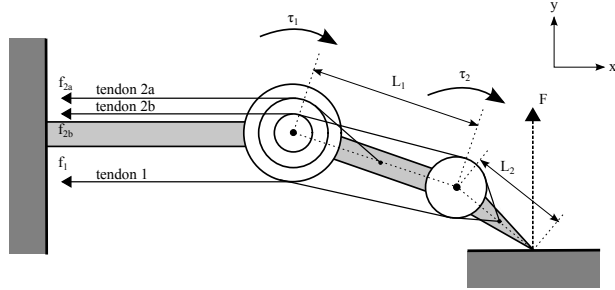


Fig. 4. Model of force equilibrium resulting from a contact with the environment.

bias force vector \mathbf{f}_b , the corresponding tendon becomes slack, as shown in Fig. 3, and the coupled motion is annulled. Using the relationships derived in this section, we develop the robotic finger in the next section. We also validate the state transition of the tendons caused by the slack of tendon in the following section.

3 Development of Robotic Finger

We produced a robotic finger with a non-elastic branching tendon and assembled two developed fingers into a two-fingered gripper. Each finger has three links and two joints with five pulleys, and is driven by flexion/extension wires.

Movement of the joints is determined by the applied torque, which is a function of the moment arm of each tendon. Therefore, the moment arm is an important factor in designing the joint movement. The finger is a simple model of a human finger, driven by branching extensor tendons and flexor tendons. Based on real parameters[14, 15], the moment arms for the robotic finger were decided as follows: $r_{11} = 7$, $r_{12} = 4$, $r_{2b1} = 3$, $r_{2b2} = 4$, $r_{2a} = 5$ (units are mm). Although the moment arm r_{2b1} is a nonlinear function of the PIP joint angle [14], we regard it as a constant for simplicity. The diameter of the pulleys was decided from real moment arms, and the link lengths also imitate those of a human finger. The lengths between joint 1 and joint 2 and between joint 2 and the fingertip are 30.5 mm and 22 mm, respectively.

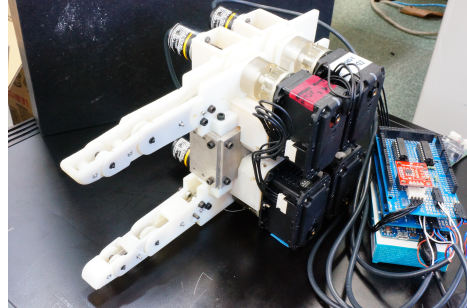


Fig. 5. Photograph of the robot hand composed of two underactuated fingers with a branching tendon

Fig. 5 shows the exterior of the finger system. Each tendon is driven by a servo motor(Dynamixel MX-64R), and the rotation angle of the base pulley that winds the tendon is measured by rotary encoders (OMRON E6A2-CW3C). This angle is used to calculate the tendon displacement. Pulses from the encoder are counted by an IC counter (NEC μ PD 4702C). The finger is controlled by Arduino DUE. Arduino - a microcontroller board that reads the values of the counter from digital input ports and outputs the commands to the motors by a serial port.

The tensile force f and tendon displacement velocity i are controlled by a winding tendon wire by the base pulley. The base pulleys are not directly connected to the servo motors, but are driven by linear-torsion springs placed between the servo motors and base pulleys. The torque exerted by the spring is calculated from the displacement difference between the base pulley and the spring; therefore, to control the tensile force on the tendon, we must control the spring displacement. The spiring constant of the selected springs is 5.17N/mm. The displacement angle of base pulley is measured by a rotary encoder directly connected to the shaft of the pulley.

The angular position and fingertip force can be controlled while the tendons do not slacken. The control is discretized, and the calculation algorithm is iterated by the micro-computer installed on Arduino. The angular position control uses a PID, which calculates the desired spring torque from the position error of a joint. The current torque of the spring is fed back to the target torque. To realize the target torque, a bias force is added to the tendon tensile force. Because the finger movement is restricted to the horizontal plane, gravity compensation is not included in the system. When not needing position control, the finger can move solely by the feedback control of the spring torque. The resulting joint torque exerts target forces on the fingertip.

Fig. 6 plots the tracking performance of the developed system. The initial response is delayed, possibly because rotational friction is exerted on the surface of the finger frame. At this stage, the gain constants are not optimally configured

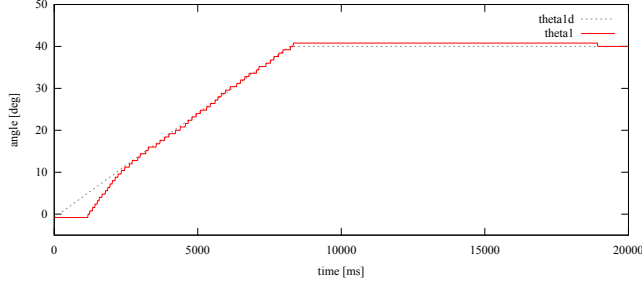


Fig. 6. Time response of joint angle 1 when the target is a ramp input. Desired angle changes from 0°-40° in approximately 8 s. Note the small time delay.

because position control is not the main focus of our research. The gains could be reconfigured in an improved design.

4 Validation of Tendon Slack

Depending on the bias tensile force of tendons and the force exerted on the fingertip, one of the branched tendons may slacken. The slacking conditions were described in Section 2. This section validates the mechanism in the real environment.

The tendon slackens when the tensile force of tendon 2a or tendon 2b in (19) becomes zero. Substituting real parameters of the robot hand into (19), we obtain

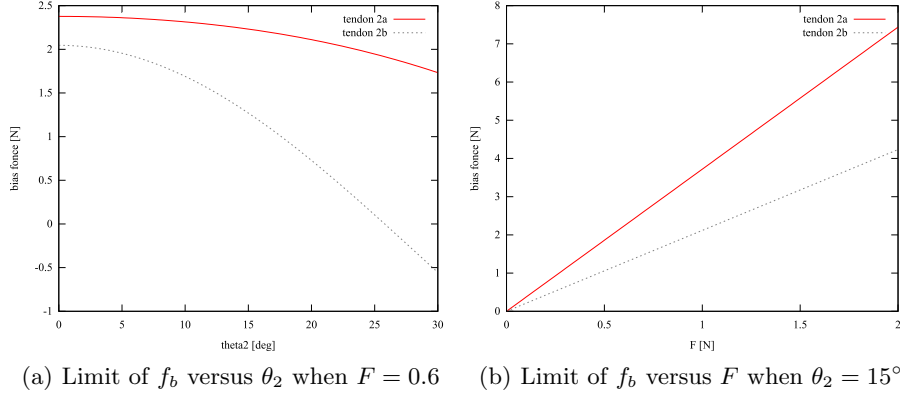
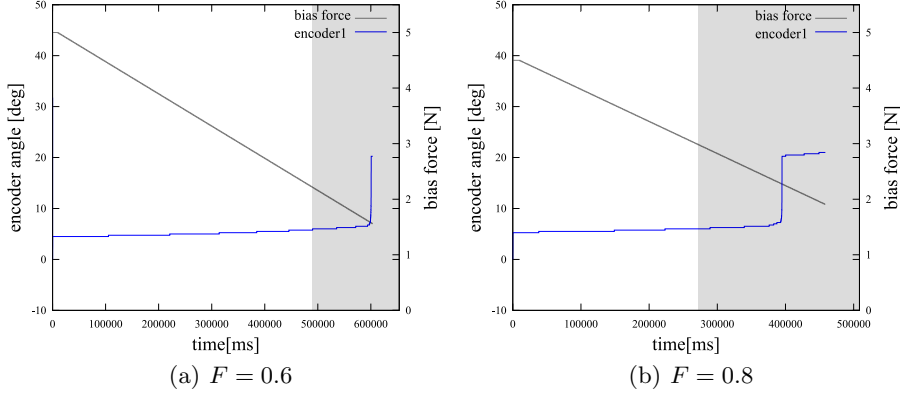
$$\begin{bmatrix} f_1 \\ f_{2b} \\ f_{2a} \end{bmatrix} = \begin{bmatrix} 0.0606L_1 \cos 2\theta_2 + 0.1098L_2 \cos 3\theta_2 \\ 0.0606L_1 \cos 2\theta_2 - 0.1402L_2 \cos 3\theta_2 \\ -0.1515L_1 \cos 2\theta_2 + 0.0387L_2 \cos 3\theta_2 \end{bmatrix} F + \begin{bmatrix} 1 \\ 1 \\ 0.8 \end{bmatrix} f_b, \quad (20)$$

where f_b is the bias tensile force variable. From (20), we can derive the f_b that renders either f_{2a} or f_{2b} zero, as a function of F and θ_2 . Fig. 7 shows the bias force f_b that retains f_{2a} and f_{2b} positive.

As shown in that figure, on the developed finger, the f_b at which f_{2a} vanishes is larger than that of f_{2b} , at any θ_2 and F . Therefore, f_{2a} falls to zero and tendon 2a loosens while f_{2b} is still positive and f_b gradually declines. To slacken tendon 2b, we must change the moment arms that define the values of the matrix P . This change requires new pulleys because the diameter of the joint pulleys decides the moment arms.

The slacking condition (20) was validated in an experiment. The bias force f_b that loosens the tendon depends on the joint angle and fingertip force F , and was experimentally determined by the following steps.

1. A large f_b was applied to retain joint coupling,
2. The finger was actuated to generate a certain fingertip force F .
3. The finger was brought into contact with a low-friction board at a specified angle θ_2 of joint 2.

(a) Limit of f_b versus θ_2 when $F = 0.6$ (b) Limit of f_b versus F when $\theta_2 = 15^\circ$ **Fig. 7.** Limiting values of f_b at which f_{2a} or f_{2b} remains positive**Fig. 8.** Result of actuation experiment at $\theta_2 = 15^\circ$

4. f_b was gradually decreased until it was sufficiently small to loosen tendon 2a.

Because the ratio of the bias force between tendons 1 and 2 is 1 : 1.8, the bias force cannot generate the joint torques and the finger remains stationary. In practice, however, the finger moves at this ratio because of the difficulty in zeroing the initial displacement of the torsion spring, and other factors. Therefore, prior to experiment, we stabilized the finger by applying a bias force at the point where the finger extends in a straight line. Here, the ratio of the bias force is the ratio of the tensile force in tendon 2 to that in tendon 1.

The actuation of the finger at joint angle $\theta_2 = 15^\circ$ and fingertip forces $F = 0.6$ and 0.8 is shown in Fig. 8. An example of finger movement throughout the experiment is shown in Fig. 9. In Fig. 8, the "bias force" is the value of f_b in (20), which is also the bias force in tendon 1. The "encoder angle" is the

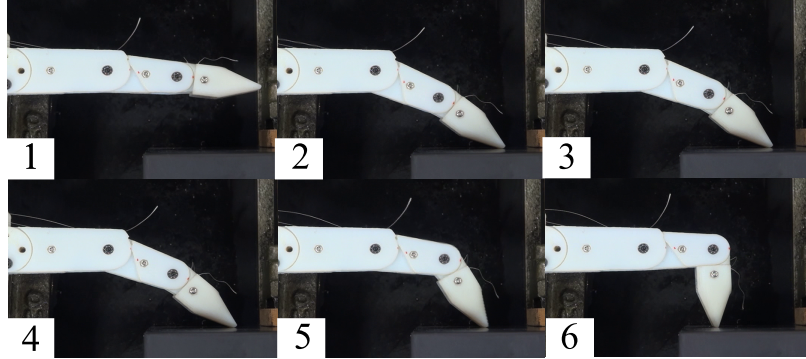


Fig. 9. Example of finger movement during the experiment. The finger moves when the bias tensile force f_b falls below the limit that retains positive tensile force in tendon 2a.

angle displacement of the drive shaft measured by the rotary encoder that drives tendon 2. The gray region is the region of negative tensile force in tendon 2a is minus. As shown in the graph, tendon 2a becomes slack and the finger movement increases the encoder value as the bias tensile force f_b falls below the limit that retains positive tensile force in tendon 2a. Thus, we have verified that the slackening of one of the branching tendons is governed by the magnitude of the bias tensile force.

In the experiment, the finger movement began at a smaller tensile force than that calculated for loosening tendon 2a. Likely, the main reason for this discrepancy is that certain environmental or other factors were ignored in deriving the condition of tendon loosening. In particular, we ignored the sliding friction between the fingertip and the board as well as the rolling friction on the joints. To account for these frictional effects, we must alter the finger's shape to accommodate both the slackening of the tendon and provision of sufficient force to overcome the friction. In this scenario, tendon relaxation would precede finger movement. In the experiment, the tendon loosened shortly before the finger slid. Hence, when controlling the finger, these effects must be considered in the robot dynamics. The another factor is the difficulty in adjusting the ratio of the bias tensile force. Changes in the bias ratio are not clearly decided because the biases are influenced by joint friction and initial position of the torsion spring. These problems are expected to be resolved with further developments of our robotic finger.

Measurement error in the link lengths and joint angles will also affect the bias tensile force. For example, if the link length is shorter than that in a real finger, the calculated bias tensile force that loosens the tendon will be overestimated. Meanwhile, the actual fingertip force is smaller than that expected because the calculated joint torque that exerts the requested force is underestimated. The smaller the fingertip force, the smaller is the required force for loosening the

tendon. Therefore, if the measured link length is shorter than the true link length, the difference between the calculated and real bias tensile forces that slacken the tendon will increase.

5 Conclusion

We have presented our two-joint robotic finger with a branching tendon. First, We produced and actuated the finger system under the position and tensile force control. Second, we found the condition under which the branched tendon loosens; in particular, when the fingertip exerts the vertical force against a plane surface. We validated this condition of the bias tensile force by experiments on the developed finger system. As a result, the force at which the tendon slackened differed between the calculated and experimental values Though, we could expect the reasons about this difference as like above discussion and intentionally loosen the branch. Our results can be an indication to actuate fingers of a gripper having a branching tendon with slack of branches.

In this paper, we cannot deal with a gripper with the developed finger. To properly use the gripper, we need to investigate grasping tactics, a control of a gripper, and so on. The non-elastic branching tendon mechanism is expected to become a notable feature in robotics, especially in anthropomorphic hand developments. In future work, further study on this mechanism is required.

References

1. Salisbury, J., Craig, J.: Articulated hands: Force control and kinematic issues. *The International Journal of Robotics Research* **1**(1) (Mar. 1982) 4–17
2. Jacobsen, S., Iversen, E., Knutti, D., Johnson, R., Biggers, K.: Design of the utah/mit dexterous hand. In: *Proceedings IEEE International Conference on Robotics and Automation*. (Apr. 1986) 1520–1532
3. Butterfass, J., Grebenstein, M., Liu, H., Hirzinger, G.: Dlr-hand ii: Next generation of a dexterous robot hand. In: *Proceedings IEEE International Conference on Robotics and Automation*. (2001) 109–114
4. Vande Weghe, M., Rogers, M., Weissert, M., Matsuoka, Y.: The act hand: design of the skeletal structure. In: *Proceedings IEEE International Conference on Robotics and Automation*. (Apr. 2004) 3375–3379
5. Birglen, L., Gosselin, C., Laliberté, T.: Underactuated robotic hands. Volume 40. Springer Verlag (2008)
6. Hirose, S., Umetani, Y.: The development of soft gripper for the versatile robot hand. *Mechanism and Machine Theory* **13**(3) (Jan. 1978) 351–359
7. Kaneko, M., Higashimori, M., Takenaka, R., Namiki, A., Ishikawa, M.: The 100 g capturing robot-too fast to see. *Mechatronics, IEEE/ASME Transactions on* **8**(1) (2003) 37–44
8. Fukaya, N., Asfour, T., Dillmann, R., Toyama, S.: Development of a Five-Finger Dexterous Hand without Feedback control: the TUAT/Karlsruhe Humanoid Hand. In: *Proceedings of the IEEE/RSJ International Conference on Intelligent Robots and Systems*. (2013) 4533–4540

9. Shirafuji, S., Ikemoto, S., Hosoda, K.: Development of a tendon-driven robotic finger for an anthropomorphic robotic hand. *The International Journal of Robotics Research* (2014) in press.
10. Sawada, D., Ozawa, R.: Joint control of tendon-driven mechanisms with branching tendons. In: Proc. IEEE Int. Conf. Robot. Autom. (May 2012) 1501–1507
11. Kobayashi, H., Hyodo, K., Ogane, D.: On tendon-driven robotic mechanisms with redundant tendons. *The International Journal of Robotics Research* **17**(5) (May 1998) 561–571
12. Murray, R., Li, Z., Sastry, S.S.: A mathematical introduction to robotic manipulation. CRC Press (1994)
13. Tsai, L.: Robot analysis: the mechanics of serial and parallel manipulators. Wiley, New York (1999)
14. Leijnse, J., Kalker, J.: A two-dimensional kinematic model of the lumbrical in the human finger. *Journal of Biomechanics* **28**(3) (Mar. 1995) 237–249
15. Spoor, C.: Balancing a force on the fingertip of a two-dimensional finger model without intrinsic muscles. *J. Biomech.* **16**(7) (1983) 497–504